· Review ·
doi: 10.13679/j.advps.2015.2.00122

Advances in Polar Science
June 2015 Vol. 26 No. 2: 122-139

Ecological controls on biogeochemical fluxes in the western Antarctic Peninsula studied with an inverse foodweb model

Hugh W. Ducklow[1*], S. C. Doney[2] & S. F. Sailley[2,3]

[1] Lamont-Doherty Earth Observatory, Columbia University, Palisades, NY, USA;

[2] Woods Hole Oceanographic Institution, Woods Hole, MA, USA;

[3] Plymouth Marine Laboratory, Plymouth, UK (Present address)

Received 5 August 2014; accepted 17 April 2015

Abstract Sea ice in the western Antarctic Peninsula (WAP) region is both highly variable and rapidly changing. In the Palmer Station region, the ice season duration has decreased by 92 d since 1978. The sea-ice changes affect ocean stratification and freshwater balance and in turn impact every component of the polar marine ecosystem. Long-term observations from the WAP nearshore and offshore regions show a pattern of chlorophyll (Chl) variability with three to five years of negative Chl anomalies interrupted by one or two years of positive anomalies (high and low Chl regimes). Both field observations and results from an inverse food-web model show that these high and low Chl regimes differed significantly from each other, with high primary productivity and net community production (NCP) and other rates associated with the high Chl years and low rates with low Chl years. Gross primary production rates (GPP) averaged 30 mmolC·m^{-2}·d^{-1} in the low Chl years and 100 mmolC·m^{-2}·d^{-1} in the high Chl years. Both large and small phytoplankton were more abundant and more productive in high Chl years than in low Chl years. Similarly, krill were more important as grazers in high Chl years, but did not differ from microzooplankton in high or low Chl years. Microzooplankton did not differ between high and low Chl years. Net community production differed significantly between high and low Chl years, but mobilized a similar proportion of GPP in both high and low Chl years. The composition of the NCP was uniform in high and low Chl years. These results emphasize the importance of microbial components in the WAP plankton system and suggest that food webs dominated by small phytoplankton can have pathways that funnel production into NCP, and likely, export.

Keywords **ecological controls, biogeochemical, food-web model**

Citation: Ducklow H W, Doney S C, Sailley S F. Ecological controls on biogeochemical fluxes in the western Antarctic Peninsula studied with an inverse foodweb model. Adv Polar Sci, 2015, 26: 122-139, doi: 10.13679/j.advps.2015.2.00122

1 Introduction

In the ocean sciences a new research agenda has emerged to delineate how foodweb structure influences the biogeochemical function of plankton systems in various regions or provinces of the global ocean[1-2]. One active area of research is determining how the magnitude and efficiency of export from the surface layer is related to plankton foodweb structure[3-5]. Plankton functional types (PFT) are often used to represent biogeochemical processes in marine ecosystem models[6-7]. PFT are defined as aggregations of particular species performing specific biogeochemical functions such as forming mineralized shells (diatoms, foraminifera), particle consumption (large and small zooplankton), and dissolved organic matter decomposition (bacteria). The simplest recognition of the PFT-based structure-function argument is the distinction between large and small phytoplankton and the foodchains they initiate[8-9]. Large phytoplankton (e.g., diatoms) are consumed by large

* Corresponding author (email: hducklow@ldeo.columbia.edu)

zooplankton (e.g., krill) and efficiently channel nutrients and energy up foodchains to top predators, and are believed to export production more efficiently to the ocean interior. Small phytoplankton (picoplankton, nanoplankton) are consumed by small grazers (e.g., protozoans and juvenile forms), retain organic matter in the surface layer, respire CO_2 and regenerate nutrients[10].

Ecological systems can be modeled as networks of compartments representing individual species, species assemblages or PFTs connected by intercompartmental flows (trophic exchanges) such as nutrient uptake, predation, excretion and respiration[11-12]. In most cases it is not possible to achieve a complete description of the structure of exchanges among compartments even in relatively simplified representations of marine ecosystems based on observations alone. This is especially true for Antarctica, where the remote location, harsh conditions and other logistic constraints limit the type, number and spatial and temporal coverage of sampling and measurements[13]. In particular, it is very difficult to assemble sufficient rate measurements defining the exchanges among key biotic groups or PFTs in Antarctic plankton foodwebs. For example, in the WAP region, there are many measurements of primary production[14-16] including size-fractionated determinations of large and small phytoplankton photosynthetic rates[17]. But measurements of new production[18], zooplankton grazing[19], bacterial production[20], and export rates[21-22] are much less common.

The Palmer LTER project, the most comprehensive observational effort in the WAP region, measures primary and bacterial production rates across the continental shelf every January[23-24], and weekly at two nearshore stations[25], but makes less frequent measurements of other key rate processes such as zooplankton grazing rates[26-27]. Critical recycling functions such as detritus production and reingestion are seldom, if ever measured.

Inverse modeling is often used to derive the most information from sparse observations[28]. An inverse model comprises a best-fit solution of flows among compartments while obeying observed exchanges, other constraints such as maximum uptake rates and other physiological rules, parameters governing rate processes, and mass conservation. This approach was first developed for geophysical systems such as defining geological strata from data on seismic wave propagation. Vézina and Platt[29] introduced the inverse method into aquatic ecology, using it to build descriptions of plankton systems in the English Channel and Celtic Sea. Subsequent efforts include diverse plankton and benthic ecosystems[30-31].

Sailley et al.[32] used an inverse model with observations from the LTER project to recover complete plankton flow networks for the WAP region. They produced a time series of model solutions for the Adélie penguin foraging regions near Anvers and Avian Islands, over the period 1995—2006. They used measurements of primary and bacterial production rates, krill standing stocks and the fraction of large versus small (< and > 20 μm) phytoplankton cells as observational constraints to their model solutions. Overall, their results reflected the great interannual variability inherent in the WAP system. The partitioning of primary production between large and small phytoplankton was the most important determinant of foodweb structure. Sailley et al's results suggest that the microbial components of the plankton system (small phytoplankton, microzooplankton and bacteria) appropriated a major part of the carbon flow in both the north and south regions, and dominated the flows in the north during most of the 1995—2006 period[32]. This conclusion notwithstanding, the krill to penguin link in the foodweb provided sufficient carbon and energy to support the estimated metabolic requirements of the penguin populations at both current and (greater) historical levels in both regions. Ballerini et al.[33] drew much the same conclusions regarding sustenance of penguin populations and the growing dominance of microbial pathways using a mass balance trophic modeling approach.

Saba et al.[25] analyzed a twenty-year time series of climate, sea ice, chlorophyll (Chl) and physical oceanographic observations from permanent nearshore sampling stations at Palmer Station (64.77ºS, 64.05ºW). They demonstrated that positive anomalies in phytoplankton and bacterial blooms occurred in years with increased winter ice extent and duration, reduced spring/summer winds, and increased water column stability in summer. Significant positive summer (December—February) Chl anomalies at Palmer Station were observed in 1996, 2002, 2006 and 2010. Analyses of penguin diet composition revealed that successful krill recruitment only occurred during the high-Chl years. Thus the WAP ecosystem is characterized by a pattern wherein physical conditions supporting large phytoplankton blooms, successful krill recruitment and enhanced food availability for foraging penguins occur every 4—6 years, separated by several years of low phytoplankton abundance, poor or nonexistent krill recruitment and less food for penguins.

Here we analyze observational data from the LTER time series and the inverse model results from Sailley et al.[32] to extend the findings of Saba et al.[25] to the regional scale, by examining the foodweb and biogeochemical flow structures associated with high and low Chl years in the north and south grid areas of the study region. We hypothesized that these annual Chl anomalies represent different foodweb states or regimes in our study region. We ask if foodwebs in high- and low Chl years (or regions) differ in structure, as reflected by different relative magnitudes of trophic exchanges and biogeochemical flows. We hypothesize that blooms of large phytoplankton, principally diatoms, drive high Chl favoring krill dominance, success of upper level predators and export (NCP). Conversely, smaller phytoplankton (cryptophytes in the WAP region: Moline et al.[34]) predominate in low Chl regimes, favoring microzooplankton, recycling and retention of biomass and nutrients in the surface layer. Some fraction of microzooplankton production is ingested by krill, providing a link between the two regimes. We pose three questions:

1. Are observations of Chl anomalies across the WAP region consistent with findings made in the nearshore region

at Palmer Station?

2. Are the inverse model results consistent with expectations for high- and low-Chl years?

3. Are contrasts in key biogeochemical processes consistent with variations in foodweb structure?

2 Methods

2.1 Study area and sampling

The Palmer LTER (PAL) study region encompasses local nearshore sampling at Palmer Station (64ºS, 64.7ºW), and a grid[35] of fixed offshore stations extending 200 km from the coast across the continental shelf, and 700 km north to south along the western Antarctic Peninsula (Figure 1). This area includes Adélie penguin rookeries and foraging areas near Palmer Station in the north, Avian Island at the southern tip of Adelaide Island, and on Charcot Island in the extreme southern part of the study region[36]. Only the Anvers and Avian regions are considered here. In this region, water depth ranges from 300 to over 1 000 m, and the summer mixed layer is 0 —50 m.

The study area is divided into cross-shelf lines of sampling stations. The lines are 100 km apart, and routinely sampled stations are spaced every 20 km along the lines (Figure 1). Every station on the 200 to 600 lines was sampled each January from 1993 through 2008. CTD-Rosette/Niskin bottle casts from the surface to the bottom and oblique zooplankton net tows (2-meter Metro net, 700 μm mesh) were performed at each of ca. 55 stations on the sampling grid[37-38]. After 2008, the sampling density was reduced to 3—4 stations per line. The grid sampling included measurements of standing stocks of bacteria, phytoplankton, macrozooplankton, physical and biogeochemical properties and primary and bacterial production rates[39-40]. Observations of Adélie penguin population size, breeding success, foraging, diet composition and recruitment were performed every October through February at Palmer Station (Anvers Island) and during a weeklong field camp at Avian Island each January[41]. Sea ice data on the annual advance, retreat, duration and extent are derived from satellite observations[42-43]. Individual results are described in publications available at http://pal.lternet.edu/publications. All data are freely accessible at http://pal.lternet.edu/data.

The extensive time series data from these projects form the foundation for the model analysis described below. Input data for the model are from the Palmer Station and RaTS sites, and the LTER offshore grid stations on the 600 lines for Anvers Island (north model region) and the 200 line for Avian Island (south model region, Figure 1). These areas comprise the Adélie penguin foraging ranges at the Anvers and Avian Island locations, respectively.

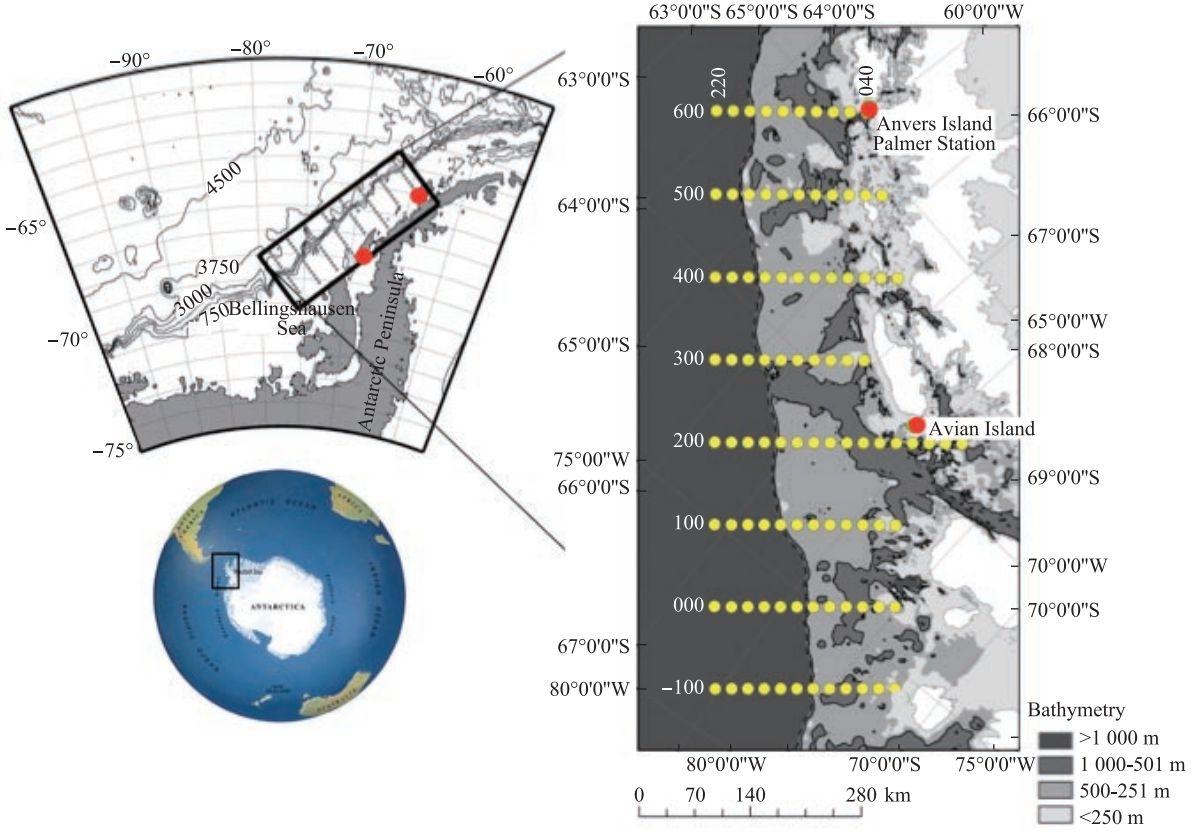

Figure 1 Map of Palmer LTER study region and sampling grid of hydrostations (yellow dots) along western Antarctic Peninsula. The offshore regions of Adélie penguin foraging areas at Anvers (North) and Avian (South) Islands (red dots) are the main focus of the modeling study.

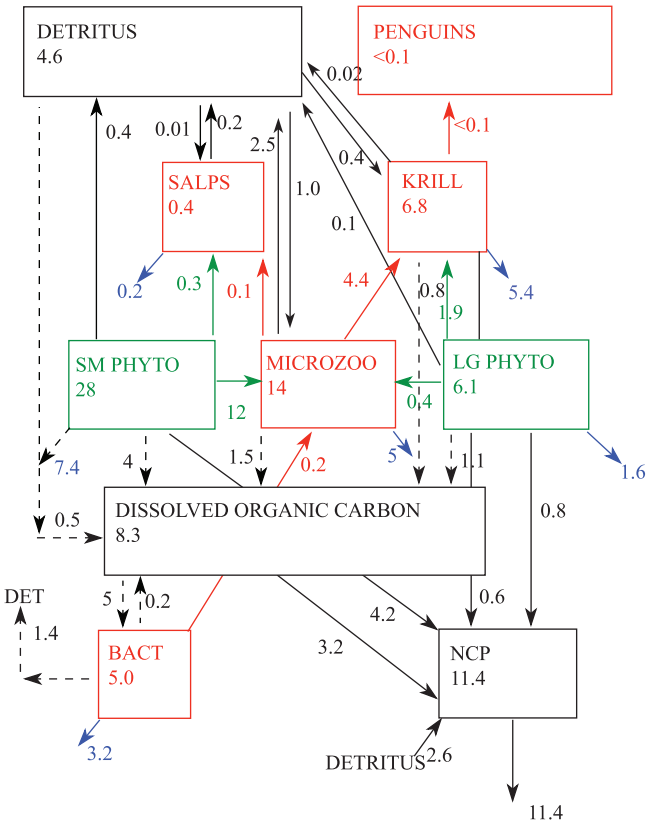

Figure 2 Intercompartmental flow diagram showing modeled foodweb for the northern (Anvers Island) Adélie penguin foraging area, in low chlorophyll anomaly years 1997, 1998 and 2004. Flows (mmolC·m^{-2}·d^{-1}) initiated by small (large) phytoplankton are on the left (right). Flows initiated by herbivores are in the top half of the diagram, and the microbial loop underneath. The numbers in the compartments are the total steady-state throughputs (sum of all inputs). Flow categories are indicated by color: black: dissolved organic carbon (dashed lines) and detrital (solid lines) flows; green: herbivory; red: secondary and higher-order consumers; blue: respiration. Abbreviations: FISH: Antarctic silverfish; SM Phyto: small phytoplankton; MICROZOO: microzooplankton; LG Phyto: large phytoplankton; BACT: bacteria; NCP: Net Community Production.

2.2 Inverse model

Sailley et al.[32] provided a new inverse model of the WAP marine foodweb using a ten-compartment system (Figure 2) with eight living (large and small phytoplankton, krill, salps, microzooplankton, fish, penguins and bacteria) and two nonliving compartments, dissolved organic carbon (DOC) and detritus. The flow currency is carbon. An eleventh external, unbalanced compartment collects unutilized carbon from the other compartments. Sailley et al. termed this the Export compartment. Here we call it Net Community Production (NCP), to avoid uncertainty as to the ultimate fate of the unutilized carbon. The model specifies 48 trophic exchanges or flows between compartments, utilizing the Markov Chain Monte Carlo (MCMC) means for each flow (Supplementary Table 1). This model does not include a mesozooplankton compartment (e.g., copepods). Sailley et al. reported on a sensitivity experiment showing that inclusion of such a compartment with observed copepod standing stocks did not change the patterns or magnitudes of flows. In the WAP in summer, mesozooplankton are about 10% of total zooplankton biomass caught in our net tows[44]. We averaged the model results (1995—2006) over years with high (> +0.5, standardized positive anomalies) and low Chl anomalies (< −0.5, standardized negative anomalies) at the north and south sites as discussed below. These average flows provide composite descriptions representing the high- and low Chl foodweb states or regimes. We also note that the inverse model provides a snapshot of the system at the time of sampling, with conditions such as temperature and available light implicit in the measured rates and biomass. Full details of model structure and solution methods are given in Sailley et al.[32].

Table 1a Annual chlorophyll values (1995—2006) for the north and south grid areas in the Palmer LTER study region along the western Antarctic Peninsula

Region / Chl anomaly	Mean Chl ± St. Dev./(ug·L^{-1})	Years/*n* (Years used in model analysis in bold)
North Low Chl	1.55±0.55	**97**,**98**,99,02,03,**04**,05 (7)
North High Chl	4.42±0.95	**95**,**96**,00,01,**06** (5)
South Low Chl	1.01±0.43	96,**97**,**98**,99,00,01,**03**,**04** (8)
South High Chl	5.37±2.99	95,**02**,05,**06** (4)

T-tests: Within regions: North High/Low $p<0.001$; South High/Low $p<0.01$; Between regions: North/south Low $p>0.05$; High $p>0.05$ (both not significant).

Table 1b Annual chlorophyll anomalies for the north and south grid areas in the Palmer LTER study region along the western Antarctic Peninsula

Region / Chl anomaly	Mean Chl anomaly ± St. Dev. /(ug·L^{-1})	Years/*n* (Years used in model analysis in bold)
North Low Chl	−0.44±0.20	**97**,**98**,99,02,03,**04**,05 (6)
North High Chl	+0.59±0.34	**95**,**96**,00,01,**06** (5)
South Low Chl	−0.43±0.23	96,**97**,**98**,99,00,01,**03**,**04** (8)
South High Chl	+1.36±1.53	95,**02**,05,**06** (4)

T-tests: Within regions: North High/Low $p<0.001$; South High/Low $p<0.01$; Between regions: North/south Low $p>0.05$; High $p>0.05$ (both not significant).

3 Results

3.1 Interannual variability in phytoplankton blooms: high vs low Chl regimes

Long-term time series with weekly resolution show that the nearshore Anvers (north) and Avian Island (south) sites are characterized by annually-occurring spring-summer phytoplankton blooms, associated with local ice retreat

and open water (Figure 3). Long-term data from the LTER offshore grid show that sea ice has alternating 4-6 year periods of high and low ice duration in the north and south (Figures 4a, 4c). Surface Chl data from each grid region show a different pattern: one or two years with positive anomalies separated by 3-5 years of negative anomalies (Figures 4b, 4d). In our study area, measured surface Chl differed significantly in high vs low Chl years (Table 1).

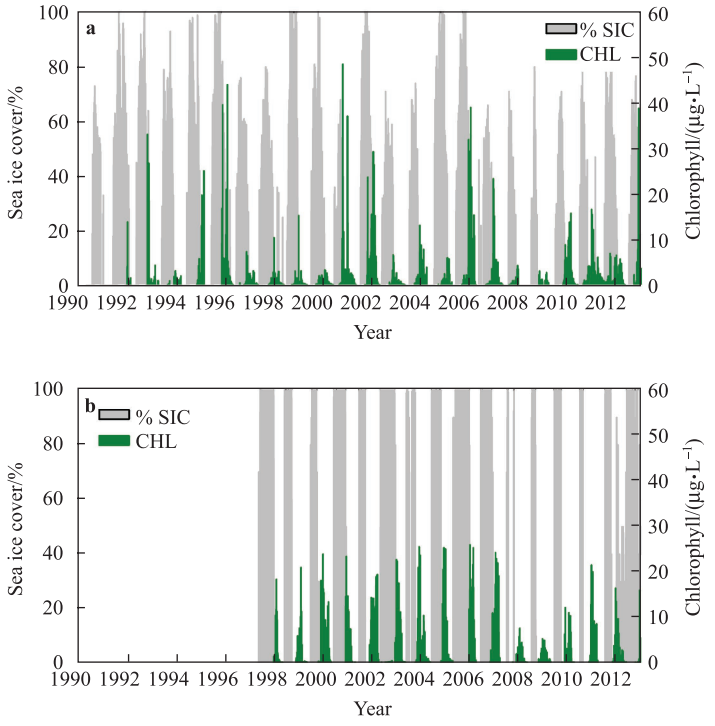

Figure 3 Nearshore time series of sea ice cover (SIC) and surface chlorophyll at Palmer Station (**a**) and Rothera Base (**b**). Palmer ice data are derived from microwave remote sensing. Rothera ice data are from local observers at the sampling site in tenths of cover (Rothera ice and Chl data courtesy H. Venables, British Antarctic Survey and RaTS-Rothera Oceanographic and Biological Time Series).

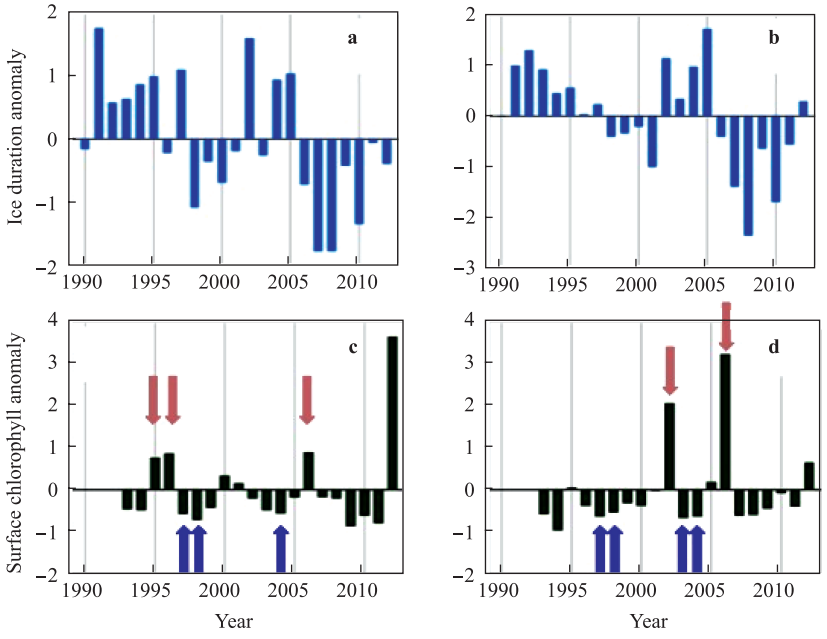

Figure 4 Standardized anomalies (*Z*-scores; 1990—2012) for sea ice duration (**a**, **b**) and surface chlorophyll (**c**, **d**) in the offshore northern (**a**,**c**) and southern (**b**, **d**) study regions. Model solutions from years with low Chl anomalies <–0.5 (blue arrows) and high (pink arrows) Chl anomalies >0.5 during 1995—2006 were averaged for analysis. Sea ice years run from March 15 of the nominal calendar year until March 14 of the next year. Chl data are from midsummer (January); thus the Chl year *X*+1 corresponds to sea ice year *X*.

3.2 Role of primary production

In the inverse model, the flow networks (e.g., Figure 2, Table S1) are initiated with input GPP values allocated to large and small phytoplankton (PPlarge and PPsmall) according to observations of size-fractionated Chl for each year from 1995—2006[23]. High GPP was clearly associated with high Chl years (Figure 5). The average GPP for the four networks in our study ranged from about 30 mmolC·m^{-2}·d^{-1} for low-Chl years in the north and south to ~100 mmolC·m^{-2}·d^{-1} for the high-Chl years (Figure 5 and Table 2). PPlarge and total GPP were each significantly different in the northern high vs low Chl years (Figure 5). In the south, the contrast between high and low Chl years resembled the north, but neither total GPP nor its components PPlarge and PPsmall differed significantly between high- and low Chl years, because of small sample sizes and high variability in the southern high Chl region in 2006 (Tables 3, 4). PPlarge and PPsmall also differed from each other significantly in the north, but not the south. There was no evidence for GPP having a greater proportion of PPlarge in high-Chl years.

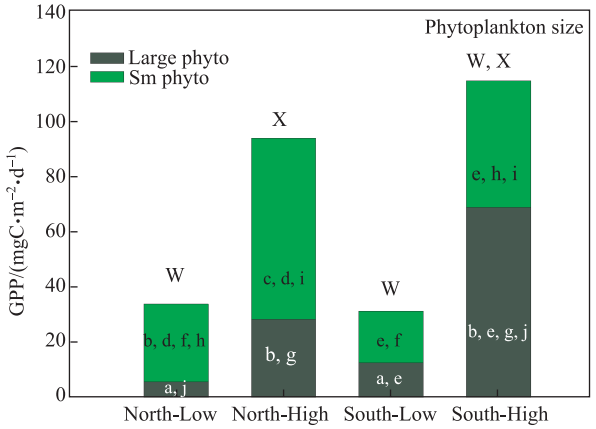

Figure 5 Distribution of model-derived gross primary production (GPP) between large and small phytoplankton in high- and low chlorophyll regimes (low and high anomalies) in the north and south study regions along the western Antarctic Peninsula. The height of the bars is the total GPP. Bars sharing the same letters are not significantly different (Mann-Whitney *U*-tests, $p>0.05$, see table 5 for data). The notation on top of the bars is for the total GPP only.

Table 2 Community metabolic rates for the inverse model solutions

Flow	North-low Chl	North-high Chl	South-low Chl	South-high Chl
PPlarge	6±5	29±4	13±6	69±72
PPsmall	28±7	65±22	19±6	46±45
GPP	34±2	94±25	32±7	115±117
NPP	25±2	69±18	23±5	85±82
CR	23±1	54±23	18±6	77±87
NCP	11±1	40±17	14±2	38±30
MIC	14±3	25±13	9±3	22±26
KRI	7±1	16±8	6±2	30±31

Note: PPlarge: gross primary production by large phytoplankton (diatoms). PPsmall: gross primary production by small phytoplankton (cryptophytes). GPP: total gross primary production (PPlarge+PPsmall). NPP: net primary production=GPP−phytoplankton respiration. CR: community respiration = sum of all respiration rates. NCP: Net community production = GPP−CR (= export from system at steady state). MIC: total ingestion by microzooplankton of all diet items (Figure 2). KRI: total ingestion by krill. All units mmolC·m^{-2}·d^{-1}.

When observations of flows associated with high and low Chl years were pooled, there were no significant differences in characteristic flows between the north and south penguin foraging regions of our study region (Figure 6a,

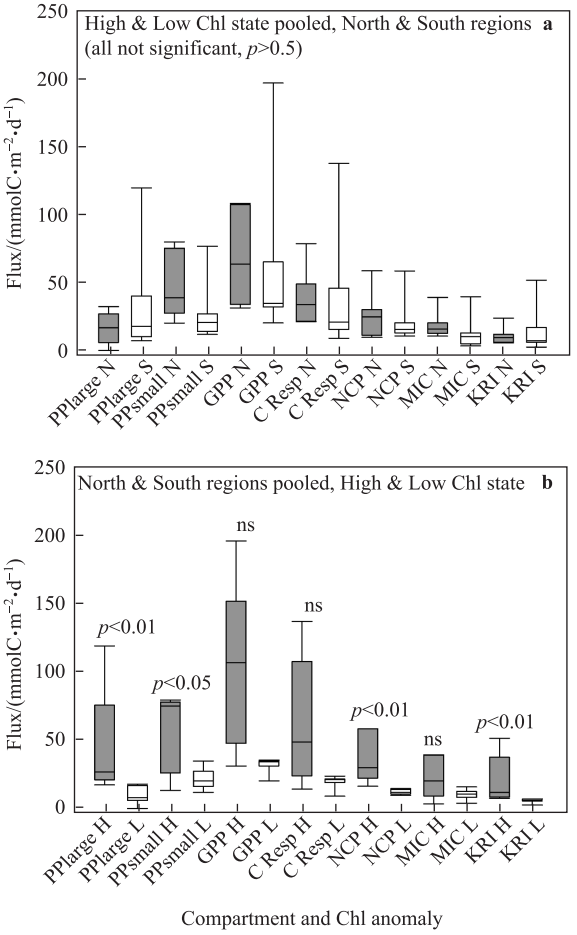

Figure 6 Box plots of selected model flows for the high- and low-Chl anomaly years in the north and south regions. **a**, High and low Chl years pooled, comparing differences between the north and south regions; **b**, North and south regions pooled, comparing differences between high and low anomaly years. In **b**, the significance level is included above pairs of samples that differed significantly (Mann-Whitney *U*-tests, ns-not significantly different, see Table 5 for data). In box plots, the box indicates the middle 75% of the data, and the bars show the 10 and 90 percentiles. The line through each box is the median.

Table 3 Comparison of inverse model intercompartmental flows in North and South study regions (Figure 6a). Years with high and low Chlorophyll anomalies (CHL) were pooled. Results (*p* values) of Mann-Whitney *U*-tests are shown at bottom of table. Abbreviations as in Table 2

Year	Region	CHL	PPlarge	PPsmall	GPP	C Resp	NCP	Micro	Kri
1995	N	H	25.54	39.57	65.11	34.46	30.65	15.72	10.10
1996	N	H	32.95	76.00	108.95	49.64	59.31	20.91	12.49
2006	N	H	27.61	80.58	108.19	79.34	28.85	39.80	24.43
1997	N	L	6.50	28.05	34.55	22.14	12.41	13.08	6.60
1998	N	L	11.13	20.81	31.94	21.77	10.17	11.19	7.67
2004	N	L	0.60	35.55	36.15	24.43	11.72	16.47	6.10
Mean	N	HL	17.39	46.76	64.15	38.63	25.52	19.53	11.23
Std Dev	N	HL	13.06	25.30	36.46	22.60	18.85	10.47	6.89
2002	S	H	17.92	13.98	31.90	14.90	17.00	3.95	8.06
2006	S	H	120.40	77.38	197.78	138.53	59.25	40.19	52.39
1997	S	L	17.37	17.65	35.02	19.70	15.32	8.67	6.55
1998	S	L	8.44	12.47	20.91	9.65	11.26	4.47	3.14
2003	S	L	7.87	27.65	35.52	22.39	13.13	12.13	6.78
2004	S	L	18.58	16.74	35.32	20.61	14.71	9.24	7.53
Mean	S	HL	31.76	27.65	59.41	37.63	21.78	13.11	14.08
Std Dev	S	HL	43.69	24.94	68.02	49.65	18.46	13.62	18.85
U-tests	N vs S	H&L	0.937 (ns)	0.065 (ns)	0.394 (ns)	0.132 (ns)	1.000 (ns)	0.093 (ns)	0.529 (ns)

Table 4 Comparison of inverse model intercompartmental flows in high and low Chlorophyll anomaly years (Figure 6b). North and South study regions were pooled. Results (p values) of Mann-Whitney *U*-tests are shown at bottom of table. Bold values are significant. Abbreviations as in Table 2

Year	Region	CHL	PPlarge	PPsmall	GPP	C Resp	NCP	Micro	Kri
1995	N	H	25.54	39.57	65.11	34.46	30.65	15.72	10.10
1996	N	H	32.95	76.00	108.95	49.64	59.31	20.91	12.49
2006	N	H	27.61	80.58	108.19	79.34	28.85	39.80	24.43
2002	S	H	17.92	13.98	31.90	14.90	17.00	3.95	8.06
2006	S	H	120.40	77.38	197.78	138.53	59.25	40.19	52.39
Mean	NS	H	44.88	57.50	102.39	63.37	39.01	24.11	21.49
Std Dev	NS	H	42.56	29.52	62.32	48.16	19.23	15.75	18.40
1997	N	L	6.50	28.05	34.55	22.14	12.41	13.08	6.60
1998	N	L	11.13	20.81	31.94	21.77	10.17	11.19	7.67
2004	N	L	0.60	35.55	36.15	24.43	11.72	16.47	6.10
1997	S	L	17.37	17.65	35.02	19.70	15.32	8.67	6.55
1998	S	L	8.44	12.47	20.91	9.65	11.26	4.47	3.14
2003	S	L	7.87	27.65	35.52	22.39	13.13	12.13	6.78
2004	S	L	18.58	16.74	35.32	20.61	14.71	9.24	7.53
Mean	NS	L	10.07	22.70	32.77	20.10	12.67	10.75	6.34
Std Dev	NS	L	6.28	8.04	5.40	4.84	1.85	3.79	1.52
U-tests	N&S	H vs L	**0.005**	**0.012**	0.073 (ns)	0.073 (ns)	**0.003**	0.149 (ns)	**0.003**

Table 3). In contrast, when the north and south regions were pooled, all the tested flow magnitudes tended to be higher in the high-Chl years (Figure 6b). However not all values were statistically different between the High- and Low-Chl years. There were significant differences between high and low Chl years for PPlarge, PPsmall, NCP, and krill ingestion (Figure 6b, Table 4). GPP, CR and microzooplankton ingestion were not significantly different between high and low Chl regimes. The latter result suggests the overall importance of microbial flows across systems in our study region, because PPsmall and microzooplankton tend to dominate the community production (e.g., Figure 5) and PPsmall, microzooplankton and bacteria are responsible for ~60% of the respiration across our study areas (Figure 8c).

3.3 Structure of trophic and biogeochemical flow networks

In addition to PPlarge and PPsmall, we focus on the total ingestion rates by microzooplankton and krill as indicators of variations in trophic (foodweb) structure, and on GPP, NCP and community respiration (CR) as indicators of biogeochemical flow structure. Variations in trophic and biogeochemical flows were driven by the total GPP as well as PPlarge and PPsmall, consistent with our hypothesis (Table 5, Figures 7, 9−11). Both microzooplankton and krill ingestion rates were significantly correlated with PPlarge (Figure 7), but the microzooplankton relationship was weaker and not correlated if the high value from the southern high-Chl anomaly year of 2006 was removed from the calculation (Table 5). Krill ingestion was significantly correlated with both PPlarge and PPsmall even when 2006

Table 5 Statistics for regressions of modeled community metabolic rates. See Figures 7, 10 for examples. Abbreviations as in Table 2

Driver group	Response group	Slope	r^2	Significance
PP large	C Resp	0.99	0.76	$p < 0.000\ 1$
PP large	NCP	0.42	0.54	$p < 0.001$
PP large	MIC	0.24	0.33	$p < 0.05$
PP large*	MIC	0.12	0.03	$p = 0.46$ (ns)
PP large	KRI	0.41	0.88	$p < 0.000\ 1$
PP small	C Resp	0.99	0.63	$p < 0.000\ 1$
PP small	NCP	0.51	0.66	$p < 0.000\ 1$
PP small	MIC	0.42	0.80	$p < 0.000\ 1$
PP small	KRI	0.30	0.40	$p < 0.001$
GPP	C Resp	0.68	0.95	$p < 0.000\ 1$
GPP	NCP	0.32	0.81	$p < 0.000\ 1$
GPP	NCP#	0.77	−27.8	$p < 0.001$
GPP	MIC	0.22	0.76	$p < 0.000\ 1$
GPP	KRI	0.24	0.86	$p < 0.000\ 1$
MIC	KRI	0.82	−0.57	$p < 0.000\ 1$

Note: * high 2006 value removed from regression; # observed data (Figure 10b).

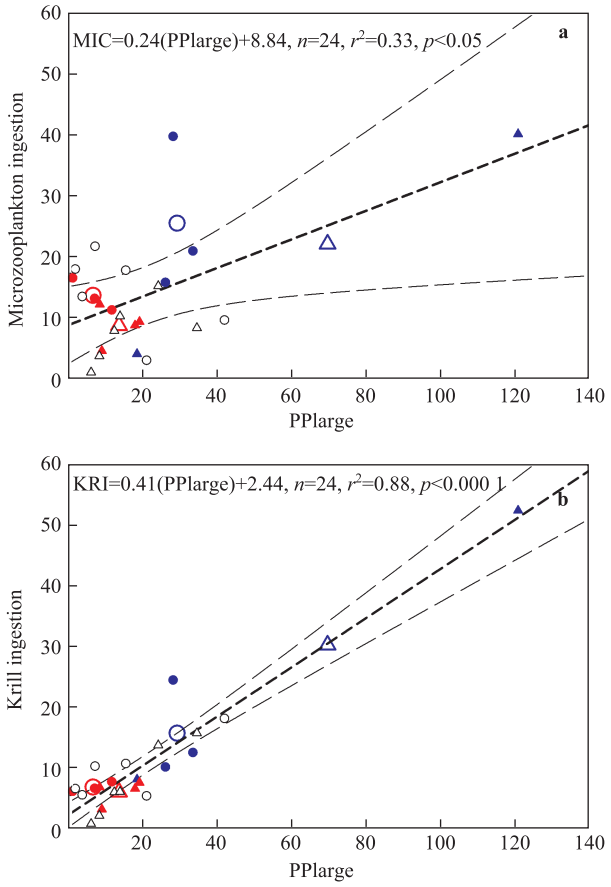

Figure 7 Regressions of modeled flows. **a**, Microzooplankton ingestion rate vs large phytoplankton production; **b**, Krill ingestion rate vs large phytoplankton production. See Figure 10 legend for explanation of plot symbols and statistics.

was not considered. The significant relationship with PPsmall (Table 5) is likely due to a significant dependence of krill ingestion on microzooplankton ingestion (Figure 9). These relationships further emphasize the importance of microbial foodweb processes across the region, and in both high- and low-Chl years. NCP was significantly correlated with GPP both in observations from 2008—2010 and in the model results for 1995—2006 (Figure 10). Community respiration and NCP were significantly correlated with PPlarge (Table 5) and PPsmall (Figure 11). The latter relationship is not consistent with our hypothesis, suggesting that the foodweb initiated with small phytoplankton has a mechanism for efficiently exporting particulate matter. This possibility is discussed further below.

3.4 Fate of GPP and other flows

The fate of the GPP summarizes the principal biogeochemical flows in an ecosystem, such that the allocation of the GPP to different processes (e.g. grazing, DOC production, respiration, Figure 8a) is a good indicator of the foodweb structure. Grazing was the most important fate for the total GPP. Grazing on small phytoplankton was the largest single

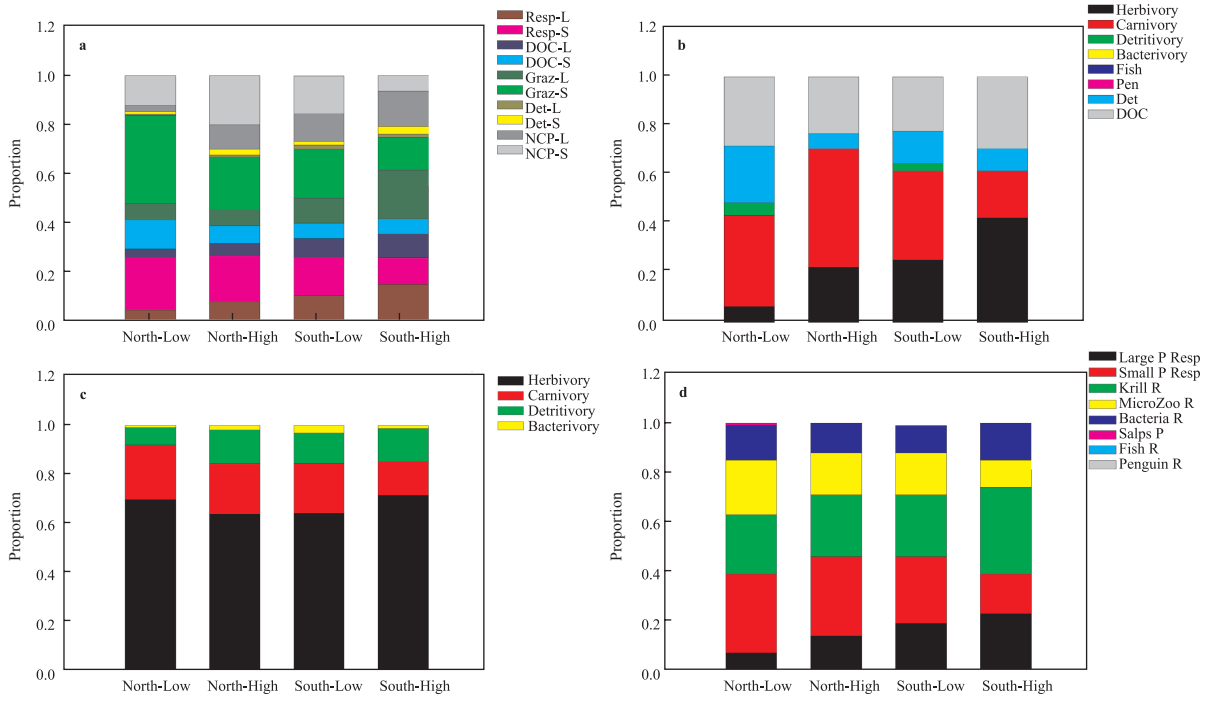

Figure 8 Components of major system level processes in high- and low chlorophyll regimes (negative and positive anomalies) in the north and south regions along the western Antarctic Peninsula. All plots normalized to the total flows in a given category and add to 100%. Groups not shown are <1% of the total. **a**, Fate of gross primary production (GPP): relative contributions of each process to the total GPP; **b**, sources of net community production; **c**, Relative contributions to total community respiration; **d**, Relative contributions to total community grazing. Abbreviations: L, S: large and small phytoplankton. R, Resp: respiration. DOC: dissolved organic matter release. Graz: grazing by krill, microzooplankton or salps. Det: losses to detritus via mortality. NCP-L, S: net community production of large and small ungrazed phytoplankton potentially available for export.

fate for GPP in northern high and low-Chl years, and in the southern low-Chl years. Even though grazing was the largest sink for the GPP, over half the total GPP was not grazed across regimes. A constant fraction (26%) of the GPP was lost to respiration across regimes, while losses to DOC and detritus together accounted for 15%—20% of the total GPP. DOC production plus microzooplankton grazing, an index of microbial foodweb activity, accounted for 43% and 56% of GPP in the high and low Chl years, respectively. In contrast, krill grazing plus ungrazed large phytoplankton, a reflection of the diatom-krill pathway, was 24% of GPP in the high Chl years in the north and south, compared to 14% in the low Chl regimes.

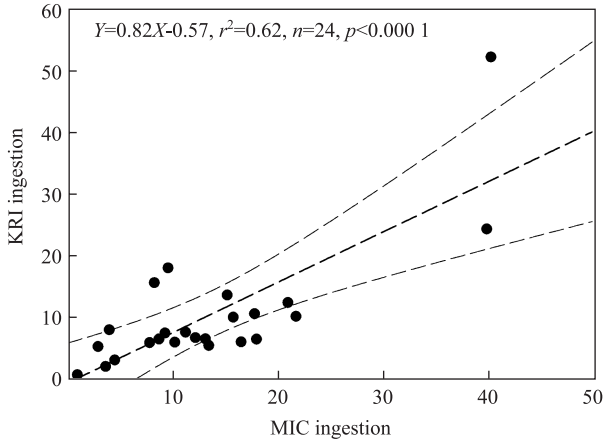

Figure 9 Regressions of modeled krill ingestion rates vs microzooplankton ingestion rates (1995—2006). The regression (dashed straight line) statistics are for all years in both regions. Curved dashed lines are 99% confidence limits.

44%—71% of the NCP was from unconsumed phytoplankton (Figure 11b), demonstrating the importance of trophic mismatch or uncoupling in the WAP system. NCP was higher in high Chl years than low (Figure 6, Table 2), but the proportion of GPP allocated to NCP was similar across the high and low Chl regimes. NCP was dominated by particle accumulation, but DOC contributed 22%—29% of the total NCP across regimes (Figure 8b).

The major grazing processes were mostly uniform across regimes (Figure 8c) and dominated by herbivory on PPsmall (Figures 8a, 8c). Community respiration was 60% heterotrophic in both high and low Chl regimes (Figure 8d). Krill and microzooplankton + bacteria each accounted for ~50% of the heterotrophic respiration in high and low Chl years.

4 Discussion

4.1 Antarctic phytoplankton blooms, biomass accumulation, and foodweb structure

Marine phytoplankton and bacteria profoundly affect

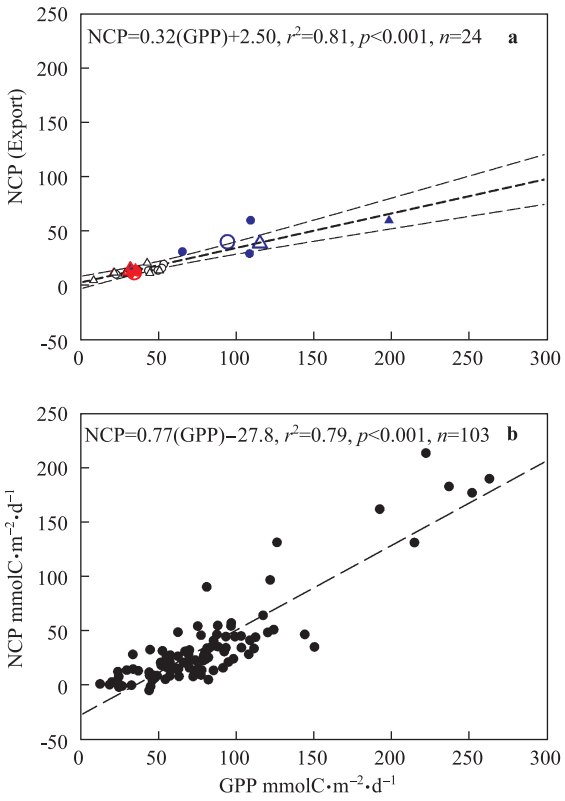

Figure 10 Regressions of modeled and observed flows. **a**, modeled NCP vs GPP, pooling all north and south region years (1995—2006). Small open circles and triangles: non-anomaly years (–0.5<X<+0.5) in the north and south regions respectively. Small filled circles and triangles: low (red) and high (blue) anomaly years in the north and south. Large red and blue open circles and triangles: means of low and high anomaly years in the north and south. The regression (dashed straight line) statistics are for all years in both regions. Curved dashed lines are 99% confidence limits. **b**, observed NCP vs GPP (2008—2010) from Huang et al.[45]

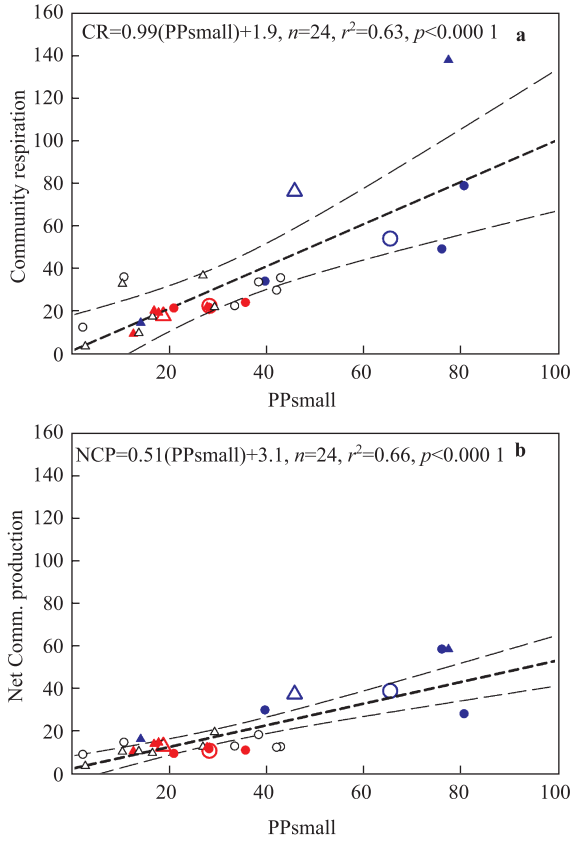

Figure 11 Regressions of modeled flows. **a**, community respiration rate vs small phytoplankton production; **b**, net community production rate vs small phytoplankton production. See Figure 10 legend for explanation of plot symbols and statistics. See Table 4 for all regression statistics.

global biogeochemical cycles[46-47]. Both theory[48-49] and marine ecosystem models[5,50-51] with sufficient complexity to embody different foodweb structures (e.g., dominance by different phytoplankton functional types and/or by large versus small cells) suggest that major biogeochemical processes such as CO_2 exchange, NCP and export are strongly influenced by variations in phytoplankton size and trophic structure. Basic theory and many observations suggest that large cells enhance particle export, while plankton ecosystems dominated by small phytoplankton cells have lower export rates and greater recycling efficiency, primarily because small particles sink more slowly and are less efficiently transferred up foodchains to larger organisms. Indeed, the diatom-dominated spring bloom in the subpolar North Atlantic has a pronounced annual export event[52] with pronounced CO_2 drawdown, whereas the oligotrophic North Pacific Subtropical Gyre has very low export[53]. In Antarctic seas, diatom blooms can efficiently strip macronutrients from the water column[54-55], affecting the elemental composition of export[56], surface layer CO_2 and air-sea gas exchange[57].

Shifts in phytoplankton community structure are associated with changes in phytoplankton standing stocks. In particular, shifts in the size distribution of Chl and GPP accompany changes in bloom magnitude. Large-celled phytoplankton (diatoms) tend to be favored during high Chl anomalies, and smaller phytoplankton (cryptophytes) dominate when Chl is lower[58-59]. Cryptophytes are also favored by local warming and increased inputs of glacial meltwater[34,60]. The overall result of these connections and changes is lower phytoplankton availability, and a larger fraction of cryptophytes in phytoplankton communities along the WAP, especially in the north[59]. Smaller cells are not efficiently filtered by krill, exacerbating the effects of lower Chl stocks for upper tropic levels.

We observed a pattern of interannual variation of Chl in the offshore region corresponding to that documented by Saba et al.[25] using the Palmer Station nearshore dataset. The similarity in the two datasets (nearshore vs offshore stations) confirms that the nearshore phytoplankton bloom records shown in Figure 3 reflect the wider regional-scale variability[23,61]. Not all regions of the WAP exhibit these

conspicuous blooms. Another nearshore long-term time series in the region demonstrates that phytoplankton blooms are strongly inhibited (Chl< 2 mg·L^{-1}) at fjordic Potter Cove, King George Island, where high summer temperatures increase water column stability, but also enhance glacial runoff containing large amounts of sediment that prevents light penetration[62]. Interannual variability of bloom magnitude at Palmer and Rothera Stations is driven by winter ice extent and spring-summer water column stability, alleviating light limitation[25,63].

In areas where large blooms occur, the amount of net production left after accounting for losses to respiration reflects the small imbalance between production and utilization in an ecosystem[64]. Although blooms may be dramatic events (Figure 3), the accumulation of ungrazed and unrespired biomass is nearly always much less than the total amount of production that could have been realized as biomass accumulation in the absence of losses[65]. Plankton ecosystems are seldom far out of balance[66-67].

Net community production is the amount of accumulated particulate and dissolved organic matter production remaining after accounting for respiratory losses[68]. Thus the NCP is a sensitive measure of ecosystem state. Model-estimated NCP rates for 1995—2006 were 11—40 mmolC·m^{-2}·d^{-1}, in the lower part of the observed range for 2008—2010[45]. NCP was 33%—43% of the model-estimated GPP, near the top end of the range derived by Huang et al.[45]. Our values are averages for the midsummer period. Direct measurements show that NCP can be negative, when community respiration exceeds the GPP, usually in the early spring and fall, or on cloudy days[67,69], but the mean condition in summer tends to be dominated by positive NCP and NCP∶GPP ratios averaging 30%[70].

Saba et al.[16] linked this pattern of interannual Chl variability (and thus primary productivity) to krill recruitment success as seen in the long-term records of diet composition of Adélie penguins foraging in the Anvers Island region. Penguin chick survival in turn is linked to foraging success[41]. These results provide a mechanistic explanation for the hypothesized regulation of long-term penguin breeding success and failure by climate variability as modulated through sea ice extent and duration, and water column stability[71]. This explanation is founded on the dynamics of the classical Antarctic diatom-krill-penguin foodchain (i.e., the large phytoplankton foodchain), a short, efficient pathway that supports a guild of large predators[72]. However, as in lower-latitude oceans, the microbial foodweb initiated by small phytoplankton, with microzooplankton grazers and bacteria, also appropriates a significant fraction of the total carbon flow in the WAP system[24,27,34,73-74]. Sailley et al.'s[23] inverse model solutions provide a detailed analysis of decadal foodweb variability of this ecosystem. Their model solutions show that the relative importance of the microbial and diatom-krill-penguin (i.e., small vs large) foodchains varies in time and space along the WAP. Importantly, the microbial foodchain is not simply a sink that detours energy away from higher trophic levels. Krill are not strictly herbivores, but can consume smaller zooplankton[75]; thus the microbial foodweb provides an important subsidy into the krill-penguin association (e.g. Figure 2).

This conceptual model does not appear to apply to Antarctic polynya regions such as the Ross and Amundsen seas, where the haptophyte *Phaeocystis antarctica* forms large blooms[76]. *Phaeocystis* has small, single-celled swarmers but also forms large multicellular colonies, blurring the distinction between small and large phytoplankton regimes. In addition, *Phaeocystis* in its large, colonial stage is not a preferred food for Antarctic krill[77].

4.2 Role of phytoplankton size and status of ecosystem change along the WAP

Along the WAP, spatial and temporal variations in Chl and primary production are governed by the advance, retreat, extent and duration of sea ice cover[23,61,78]. The WAP region is currently experiencing rapid and significant regional warming on an annual basis and especially in winter[79-81]. A major consequence and driver[82] of this warming has been loss of sea-ice cover, manifested in later dates of advance, earlier retreat, and consequent declines in extent and duration[43,83]. Moreover, there is a pronounced gradient of ice cover along the WAP, with longer duration and greater extent in the south and shorter duration and lesser extent in the north (Figure 3). The LTER study region (Figure 1) along the WAP now experiences roughly 100 d less ice cover than at the beginning of the satellite record in 1978.

As a result of these changes, the magnitude of primary production and phytoplankton community composition are also changing in space and time, with consequences for plankton foodweb and biogeochemical dynamics and higher trophic levels[84]. In the north, lower winter ice extent is associated with weaker water column stability in the spring. This change in ocean mixed layer climate is associated with lower Chl (and thus, lower production rates) during the spring bloom[25,59,63].

Our inverse model results are not so clear as earlier surveys and model generalizations may suggest. Phytoplankton productivity was clearly associated with high Chl in observations and models. The relative importance of major biogeochemical processes such as grazing, DOC cycling and NCP were more or less uniform across the north and south, and in high and low Chl years. In particular, NCP, the major determinant of export magnitude, was the same fraction (30%—40%) of the total GPP in the high and low Chl years. Notably, the NCP fraction of GPP remained the same even when it was dominated by small phytoplankton (Figures 8a, 8b). These results suggest that a foodweb characterized by smaller phytoplankton may be equally efficient at exporting production as a large-phytoplankton system. In the Equatorial Pacific, another inverse model analysis showed that the role of small cells in the export was directly proportional to their abundance in the productive layer[30,85].

In other words, larger, more rapidly-sinking phytoplankton (particularly dense, mineralized forms like diatoms) did not have a disproportionate effect on export, although Stukel and Landry[86] suggested that result may have been a consequence of assumptions underlying their model. Observations along the WAP also support the hypothesis that smaller cells can contribute importantly to the export. The highest NCP estimates in 2008 in the LTER study region were at stations dominated by cryptophytes, not diatoms[45]. This may be because microzooplankton funnel small phytoplankton production into krill and salps that produce rapidly-sinking fecal pellets[87] (Figure 8).

5 Summary

Long term observations in the north and south offshore regions of the study region showed a characteristic pattern of Chl variability: four to six years of negative Chl anomalies interrupted by one-two years of positive anomalies, consistent with an established pattern observed in the nearshore region at Palmer Station (Question 1 in Introduction). Time series results (1995—2006) from an inverse foodweb model were examined to test if patterns of major trophic flows (size-dependent primary production and grazing rates) and biogeochemical fluxes (gross primary and net community production and community respiration rates) were consistent with hypotheses about foodweb dynamics in high- and low-Chl years.

There were no significant differences between corresponding model flows in the north and south regions of the study area; however, primary production by large and small phytoplankton, community respiration and krill ingestion rates differed significantly between high- and low-Chl years, consistent with expectations about foodweb trophic and biogeochemical dynamics (Question 2). In contrast, the patterns of relative flow magnitudes such as the ratio of NCP to GPP or the sources of community respiration and fates of GPP were similar between high and low Chl years, contradicting our hypothesis about the dependence of biogeochemical processes on phytoplankton size (Question 3). It is possible that these results are the result of small sample sizes, and that a longer model or observational time series will show clearer patterns.

Several observations supported the recently recognized importance of microbial processes in Antarctic waters. Krill ingestion was significantly correlated with microzooplankton ingestion rates, and with small phytoplankton productivity. Large and small phytoplankton production rates were similar in high and low Chl years, as were krill and microbial respiration rates. These results suggest that foodwebs dominated by small phytoplankton can have pathways that funnel production into NCP, and likely, export.

Acknowledgments This research was supported by NSF Polar Programs awards ANT-1344502 and PLR-1440435 to HWD at Lamont-Doherty Earth Observatory. SFS and SCD were supported partly by Woods Hole Oceanographic Institution. We are grateful for data and discussions with our Palmer LTER colleagues, including K. Huang, K. Bernard, G. Saba, O. Schofield, S. Stammerjohn, D. Steinberg, and W. Fraser; and BAS-RaTS colleagues M. Meredith and H. Venables.

References

1 Boyd P W, Doney S C. Modelling regional responses by marine pelagic ecosystems to global climate change. Geophys Res Lett, 2002, 29(16): 531–534, doi: 1810.1029/2001GL014130
2 Falkowski P G, Laws E A, Barber R T, et al. Phytoplankton and their role in primary, new, and export production// Fasham M J R. Ocean biogeochemistry: the role of the ocean carbon cycle in global change. Berlin Heidelberg: Springer, 2003: 99–121
3 Boyd P W, Newton P P. Does planktonic community structure determine downward particulate organic carbon flux in different oceanic provinces? Deep-Sea Res I, 1999, 46(1): 63–91
4 Longhurst A R, Harrison W G. The biological pump: Profiles of plankton production and consumption in the upper ocean. Progr Oceanogr, 1989, 22(1): 47–123
5 Siegel D A, Buesseler K O, Doney S C, et al. Global assessment of ocean carbon export by combining satellite observations and food-web models. Global Biogeochem Cycles, 2014, 28(3): 181–196, doi: 10.1002/2013GB004743
6 Le Quéré C, Harrison S P, Prentice I C, et al. Ecosystem dynamics based on plankton functional types for global ocean biogeochemistry models. Global Change Biol, 2005, 11(11): 2016–2040
7 Moore J K, Doney S C, Lindsay K. Upper ocean ecosystem dynamics and iron cycling in a global 3-D model. Global Biogeochem Cycles, 2004, 18: GB4028
8 Malone T C. The relative importance of nannoplankton and netplankton as primary producers in tropical oceanic and neritic phytoplankton communities. Limnol Oceanogr, 1971, 16(4): 633–639
9 Barber R T. Ocean basin ecosystems// Alberts J , Pomeroy L R. Concepts of ecosystem ecology: a comparative view. New York: Springer, 1988
10 Ducklow H W. Chapter 1. Biogeochemical Provinces: Towards a JGOFS Synthesis// Fasham M J R. Ocean biogeochemistry: a new paradigm. New York: Springer-Verlag, 2003: 3–18
11 Odum H T, Odum E P. Trophic structure and productivity of a windward coral reef community on eniwetok atoll. Ecolog Monogr, 1955, 25(3): 291–320
12 Fasham M J R. Flow analysis of materials in the marine euphotic zone. Can Bull Fish Aquat Sci, 1985, 213: 139–162
13 Schofield O, Ducklow H W, Martinson D G, et al. How do polar marine ecosystems respond to rapid climate change? Science, 2010, 328(5985): 1520–1523
14 Schloss I R, Wasilowska A, Dumont D, et al. On the phytoplankton bloom in coastal waters of southern King George Island (Antarctica) in January 2010: An exceptional feature? Limnol Oceanogr, 2014, 59(1): 195–210
15 Holm-Hansen O, Mitchell B G. Spatial and temporal distribution of phytoplankton and primary production in the western Bransfield Strait region. Deep-Sea Res A, 1991, 38(8–9): 961–980
16 Lorenzo L M, Arbones B, Figueiras F G, et al. Photosynthesis, primary production and phytoplankton growth rates in Gerlache and Bransfield Straits during Austral summer: cruise FRUELA 95. Deep-Sea Res II, 2002, 49(4–5): 707–721
17 Varela M, Fernandez E, Serret P. Size-fractionated phytoplankton biomass and primary production in the Gerlache and south Bransfield Straits (Antarctic Peninsula) in Austral summer 1995–1996. Deep-Sea

Res II, 2002, 49(4–5): 749–768
18 Bode A, Castro C G, Doval M D, et al. New and regenerated production and ammonium regeneration in the western Bransfield Strait region (Antarctica) during phytoplankton bloom conditions in summer. Deep-Sea Res II, 2002, 49(1): 787–804
19 Cabal J A, Alvarez-Marqués F, Acuña J L, et al. Mesozooplankton distribution and grazing during the productive season in the Northwest Antarctic Peninsula (FRUELA cruises). Deep-Sea Res II, 2002, 49(4–5): 869–882
20 Morán X A G, Gasol J M, Pédros-Alió C, et al. Dissolved and particulate primary production and bacterial production in offshore Antarctic waters during Austral summer: coupled or uncoupled? Mar Ecol Progr Ser, 2001, 222: 25–39
21 Anadón R, Alvarez-Marqués F, Fernández E, et al. Vertical biogenic particle flux during Austral summer in the Antarctic Peninsula area. Deep-Sea Res II, 2002, 49(4–5): 883–901
22 Karl D M, Tilbrook B D, Tien G. Seasonal coupling of organic matter production and particle flux in the western Bransfield Strait, Antarctica. Deep-Sea Res, 1991, 38(8–9): 1097–1126
23 Vernet M, Martinson D, Iannuzzi R, et al. Primary production within the sea-ice zone west of the Antarctic Peninsula: I-Sea ice, summer mixed layer, and irradiance. Deep-Sea Res II, 2008, 55(18–19): 2068–2085
24 Ducklow H W, Schofield O, Vernet M, et al. Multiscale control of bacterial production by phytoplankton dynamics and sea ice along the western Antarctic Peninsula: A regional and decadal investigation. J Mar Syst, 2012, 98–99: 26–39
25 Saba G K, Fraser W R, Saba V S, et al. Winter and spring controls on the summer food web of the coastal West Antarctic Peninsula. Nat Commun, 2014, 5, doi: 10.1038/ncomms5318
26 Bernard K S, Steinberg D K, Schofield O M E. Summertime grazing impact of the dominant macrozooplankton off the Western Antarctic Peninsula. Deep-Sea Res I, 2012, 62: 111–122
27 Garzio L M, Steinberg D K, Erickson M, et al. Microzooplankton grazing along the Western Antarctic Peninsula. Aqu Microb Ecol, 2013, 70(3): 215–232
28 Glover D M, Jenkins W J, Doney S C. Modeling methods for marine science. Cambridge, UK: Cambridge University Press, 2011
29 Vézina A F, Platt T. Food web dynamics in the ocean. I. Best-estimates of flow networks using inverse methods. Mar Ecol Progr Ser, 1988, 42: 269–287
30 Richardson T L, Jackson G A. Small phytoplankton and carbon export from the surface ocean. Science, 2007, 315(5813): 838–840
31 van Oevelen D, Van den Meersche K, Meysman F J R, et al. Quantifying food web flows using linear inverse models. Ecosystems, 2010, 13(1): 32–45
32 Sailley S F, Ducklow H W, Moeller H V, et al. Carbon fluxes and pelagic ecosystem dynamics near two western Antarctic Peninsula Adélie penguin colonies: an inverse model approach. Mar Ecol Progr Ser, 2013, 492: 253–272
33 Ballerini T, Hofmann E E, Ainley D G, et al. Productivity and linkages of the food web of the southern region of the western Antarctic Peninsula continental shelf. Progr Oceanogr, 2014, 122: 10–29
34 Moline M A, Claustre H, Frazer T K, et al. Alteration of the food web along the Antarctic Peninsula in response to a regional warming trend. Global Change Biol, 2004, 10(12): 1973–1980
35 Waters K J, Smith R C. Palmer LTER: A sampling grid for the Palmer LTER program. Antarct J United States, 1992, 27(5): 236–239
36 Schofield O, Ducklow H, Bernard K S, et al. Penguin biogeography along the West Antarctic Peninsula: Testing the canyon hypothesis with Palmer LTER observations. Oceanography, 2013, 26: 78–80
37 Ross R M, Quetin L B, Martinson D G, et al. Palmer LTER: Patterns of distribution of five dominant zooplankton species in the epipelagic zone west of the Antarctic Peninsula, 1993–2004. Deep-Sea Res II, 2008, 55(18–19): 2086–2105
38 Martinson D G, Stammerjohn S E, Iannuzzi R A, et al. Western Antarctic Peninsula physical oceanography and spatio-temporal variability. Deep-Sea Res II, 2008, 55(18–19): 1964–1987
39 Ross R M, Hofmann E E, Quetin L B. Foundations for ecological research west of the Antarctic Peninsula. Washington, DC: American Geophysical Union, 1996
40 Ducklow H W, Baker K, Martinson D G, et al. Marine ecosystems: The West Antarctic Peninsula. Philosoph Trans Roy Soc London B, 2007, 362(1477): 67–94
41 Fraser W R, Hofmann E E. A predator's perspective on causal links between climate change, physical forcing and ecosystem response. Mar Ecol Progr Ser, 2003, 265: 1–15
42 Stammerjohn S E, Smith R C. Spatial and temporal variability of western Antarctic peninsula sea ice coverage// Ross R M, Hofmann E E, Quetin L B. Foundations for ecological research west of the Antarctic Peninsula. Washington, DC: American Geophysical Union, 1996: 81–104
43 Stammerjohn S E, Martinson D G, Smith R C, et al. Sea ice in the western Antarctic Peninsula region: Spatio-temporal variability from ecological and climate change perspectives. Deep-Sea Res II, 2008, 55(18–19): 2041–2058
44 Steinberg D K, Ruck K E, Gleiber M R, et al. Long-term (1993–2013) changes in macrozooplankton off the Western Antarctic Peninsula. Deep-Sea Res I, 2015, 101: 54–70
45 Huang K, Ducklow H, Vernet M, et al. Export production and its regulating factors in the West Antarctica Peninsula region of the Southern Ocean. Global Biogeochem Cycles, 2012, 26(2): 0886-6236, doi: 10.1029/2010GB004028
46 Arrigo K R. Marine microorganisms and global nutrient cycles. Nature, 2005, 437(7057): 349–355
47 Falkowski P G, Fenchel T, Delong E F. The microbial engines that drive Earth' s biogeochemical cycles. Science, 2008, 320(5879): 1034–1039
48 Falkowski P G, Barber R T, Smetacek V. Biogeochemical controls and feedbacks on ocean primary production. Science, 1998, 281(5374): 200–206
49 Falkowski P G, Oliver M J. Mix and match: how climate selects phytoplankton. Nat Rev Microbiol, 2007, 5(10): 813–819
50 Laws E A, Falkowski P G, Smith W O, et al. Temperature effects on export production in the open ocean. Global Biogeochem Cycles, 2000, 14(4): 1231–1246
51 Moore J K, Lindsay K, Doney S C, et al. Marine ecosystem dynamics and biogeochemical cycling in the Community Earth System Model. J Climate, 2013, 26(23): 9291–9321
52 Billett D S M, Lampitt R S, Rice A L, et al. Seasonal sedimentation of phytoplankton to the deep-sea benthos. Nature, 1983, 302(5908): 520–522
53 Karl D M. A sea of change: biogeochemical variability in the North Pacific Subtropical Gyre. Ecosystems, 1999, 2(3): 181–214
54 Smith W O, Nelson D M. Phytoplankton bloom produced by a receding ice edge in the Ross Sea: spatial coherence with the density field. Science, 1985, 227(4683): 163–166
55 Jennings J C, Gordon L I, Nelson D M. Nutrient depletion indicates high primary productivity in the Weddell Sea. Nature, 1984, 309(5963): 51–54
56 Arrigo K R, Robinson D H, Worthen D L, et al. Phytoplankton

community structure and the drawdown of nutrients and CO2 in the Southern Ocean. Science, 1999, 283(5400): 365–367
57 Montes-Hugo M, Sweeney C, Doney S C, et al. Seasonal forcing of summer dissolved inorganic carbon and chlorophyll *a* on the Western Shelf of the Antarctic Peninsula. J Geophys Res-Oceans, 2010, 115(C3), doi: 10.1029/2009JC005267
58 Montes-Hugo M A, Vernet M, Martinson D, et al. Variability on phytoplankton size structure in the western Antarctic Peninsula (1997–2006). Deep-Sea Res II, 2008, 55(18–19): 2106–2117
59 Montes-Hugo M, Doney S C, Ducklow H W, et al. Recent changes in phytoplankton communities associated with rapid regional climate change along the western Antarctic Peninsula. Science, 2009, 323(5920): 1470–1473
60 Dierssen H M, Smith R C, Vernet M. Glacial meltwater dynamics in coastal waters West of the Antarctic Peninsula. Proc Natl Acad Sci USA, 2002, 99(4): 1790–1795
61 Smith R C, Martinson D G, Stammerjohn S E, et al. Bellingshausen and western Antarctic Peninsula region: Pigment biomass and sea-ice spatial/temporal distributions and interannual variabilty. Deep-Sea Res II, 2008, 55(18–19): 1949–1963
62 Schloss I R, Abele D, Moreau S, et al. Response of phytoplankton dynamics to 19-year (1991–2009) climate trends in Potter Cove (Antarctica). J Mar Syst, 2012, 92(1): 53–66
63 Venables H J, Clarke A, Meredith M P. Wintertime controls on summer stratification and productivity at the Western Antarctic Peninsula. Limnol Oceanogr, 2013, 58(3): 1035–1047
64 Longhurst A. Seasonal cycles of pelagic production and consumption. Progr Oceanogr, 1995, 36(2): 77–167
65 Behrenfeld M J. Climate-mediated dance of the plankton. Nat Climate Change, 2014, 4(10): 880–887
66 Longhurst A. Ecological geography of the sea. San Diego, CA: Academic Press, 1998
67 Tortell P D, Asher E C, Ducklow H W, et al. Metabolic balance of coastal Antarctic waters revealed by autonomous pCO2 and ΔO2/Ar measurements. Geophys Res Lett, 2014, 41(19): 6803–6810
68 Ducklow H W, Doney S C. What is the metabolic state of the oligotrophic ocean? A debate. Ann Rev Mar Sci, 2013, 5: 525–533
69 Williams P J B, Quay P D, Westberry T K, et al. The oligotrophic ocean is autotrophic. Ann Rev Mar Sci, 2013, 5: 535–549
70 Quay P D, Peacock C, Björkman K, et al. Measuring primary production rates in the ocean: Enigmatic results between incubation and non-incubation methods at Station ALOHA. Global Biogeochem Cycles, 2010, 24(3): GB3014
71 Smith R C, Fraser W R, Stammerjohn S E. Climate variability and ecological response of the marine ecosystem in the western Antarctic Peninsula (WAP) region // Greenland D, Goodin D G, Smith R C. Climate variability and ecosystem response at Long-Term Ecological Research Sites. New York: New York Oxford University Press, 2003: 158–173
72 Knox G A. Biology of the Southern Ocean. Boca Raton, FL: CRC Press, 2006
73 Garzio L M, Steinberg D K. Microzooplankton community composition along the Western Antarctic Peninsula. Deep-Sea Res I, 2013, 77: 36–49
74 Vaqué D, Guixa-Boixereu N, Gasol J M, et al. Distribution of microbial biomass and importance of protists in regulating prokaryotic assemblages in three areas close to the Antarctic Peninsula in spring and summer 1995/96. Deep-Sea Res II, 2002, 49(4–5): 847–867
75 Atkinson A, Snÿder R. Krill-copepod interactions at South Georgia, Antarctica, I. Omnivory by Euphausia superba. Mar Ecol Progr Ser, 1997, 160: 63–76
76 Arrigo K R, van Dijken G L. Phytoplankton dynamics within 37 Antarctic coastal polynya systems. J Geophys Res, 2003, 108(C8), doi: 10.1029/2002JC001739
77 Leventer A, Dunbar R B. Factors influencing the distribution of diatoms and other algae in the Ross Sea. J Geophys Res, 1996, 101(C8): 18489–18500
78 Schloss I R, Ferreyra G A, Ruiz-Pino D. Phytoplankton biomass in Antarctic shelf zones: a conceptual model based on Potter Cove, King George Island. J Mar Syst, 2002, 36(3–4): 129–143
79 Vaughan D G, Marshall G J, Connolley W M, et al. Recent rapid regional climate warming on the Antarctic Peninsula. Climatic Change, 2003, 60(3): 243–274
80 Meredith M P, King J C. Rapid climate change in the ocean west of the Antarctic Peninsula during the second half of the 20th century. Geophys Res Lett, 2005, 32(19), doi: 10.1029/2005GL024042
81 Turner J, Bindschadler R A, Convey P, et al. Antarctic climate change and the environment. Cambridge UK: Scientific Committee for Antarctic Research, 2009
82 Turner J, Maksym T, Phillips T, et al. The impact of changes in sea ice advance on the large winter warming on the western Antarctic Peninsula. Int J Climatol, 2013, 33(4): 852–861
83 Stammerjohn S E, Martinson D G, Smith R C, et al. Trends in Antarctic annual sea ice retreat and advance and their relation to ENSO and southern annular mode variability. J Geophys Res, 2008, 113(C3), doi: 10.1029/2007JC004269
84 Moline M A, Karnovsky N J, Brown Z, et al. High latitude changes in ice dynamics and their impact on polar marine ecosystems. Ann New York Acad Sci, 2008, 1134: 267–319
85 Richardson T L, Jackson G A, Ducklow H W, et al. Carbon fluxes through food webs of the eastern equatorial Pacific: an inverse approach. Deep-Sea Res I, 2004, 51(9): 1245–1274
86 Stukel M R, Landry M R. Contribution of picophytoplankton to carbon export in the equatorial Pacific: A re-assessment of food-web flux inferences from inverse models. Limnol Oceanogr, 2010, 55(6): 2669–2685
87 Gleiber M R, Steinberg D K, Ducklow H W. Time series of vertical flux of zooplankton fecal pellets on the continental shelf of the western Antarctic Peninsula. Mar Ecol Progr Ser, 2012, 471: 23–36

Supplementary Table 1 Summary of averaged intercompartmental flows for inverse model solutions for North region. Flows were averaged over high- and low-Chl anomaly years as shown in Figure 4. Flow units mmolC·m^{-2}·d^{-1} and normalized to the total Gross Primary Production (GPP). The FISH compartment is not included in the North region. Flows > 5% GPP are highlighted in bold.

North Region	**Negative Chlorophyll nomalies**			**Positive hlorophyll nomalies**		
Compartment	**Throughput**		**Norm GPP**	**Throughput**		**Norm GPP**
PPlarge	6.08		0.18	28.70		0.31
PPsmall	28.14		0.82	65.38		0.69
Mic	13.58		0.40	25.48		0.27
Kri	6.79		0.20	15.67		0.17
Fish	na		na	na		na
Pen	0.004		0.00	0.004		0.00
Det	4.61		0.13	8.90		0.09
DOC	8.28		0.24	17.23		0.18
Bac	5.05		0.15	8.26		0.09
Sal	0.39		0.01	0.05		0.00
Exp	11.43		0.33	39.61		0.42
Flow	**Avg flow**	**SD low**	**Norm GPP**	**Avg flow**	**SD Flow**	**Norm GPP**
PhyL to mic	0.43	0.38	0.01	1.42	0.29	0.02
PhyS to mic	11.94	2.97	**0.35**	20.01	13.42	**0.21**
Det to Mic	1.04	0.17	0.03	3.32	1.20	0.04
Bac to Mic	0.17	0.02	0.00	0.73	0.52	0.01
DOC to Bac	5.05	0.31	**0.15**	8.26	6.15	**0.09**
PhyL to Lkri	1.92	1.72	**0.06**	4.85	4.30	**0.05**
Mic to kri	4.44	0.89	**0.13**	8.46	4.60	**0.09**
Det to Kri	0.43	0.09	0.01	2.36	1.65	0.03
PhyS to sal	0.27	0.27	0.01	0.04	0.06	0.00
Mic to sal	0.11	0.10	0.00	0.01	0.02	0.00
Det to Sal	0.01	0.01	0.00	0.00	0.00	0.00
Bac to Sal	0.01	0.01	0.00	0.00	0.00	0.00
Kri to Pen	0.00	0.00	0.00	0.00	0.00	0.00
Fish to pen	na	na	na	na	na	na
Kri to fish	na	na	na	na	na	na
Resp phL	1.63	1.42	**0.05**	7.64	0.79	**0.08**
Resp phS	7.36	1.93	**0.22**	17.65	6.10	**0.19**
Resp bac	3.24	0.31	**0.09**	6.45	6.15	**0.07**
Resp mic	5.00	1.07	**0.15**	9.29	4.96	0.10
Resp sal	0.17	0.17	0.00	0.02	0.03	0.00
Resp kri	5.39	0.79	**0.16**	13.43	6.97	**0.14**
Resp pen	0.00	0.00	0.00	0.00	0.00	0.00

(To be continued)

(Continued)

Resp Fish	na	na	na	na	na	na
PhL to DOC	1.14	0.99	0.03	4.72	0.60	**0.05**
PhS to DOC	3.99	1.12	**0.12**	6.58	5.62	**0.07**
Bac to DOC	0.22	0.03	0.01	0.38	0.26	0.00
Mic to DOC	1.52	0.28	0.04	2.86	1.29	0.03
Sal to DOC	0.07	0.06	0.00	0.01	0.01	0.00
Kri to DOC	0.82	0.06	0.02	1.91	0.85	0.02
Pen to DOC	0.00	0.00	0.00	0.00	0.00	0.00
Fish to DOC	na	na	na	na	na	na
Det to DOC	0.53	0.07	0.02	0.78	0.21	0.01
PhL to Det	0.13	0.11	0.00	0.87	0.51	0.01
PhS to Det	0.38	0.20	0.01	2.22	2.10	0.02
Bac to Det	1.41	0.05	0.04	0.70	0.78	0.01
Mic to Det	2.52	0.40	**0.07**	4.86	1.84	**0.05**
Salp to Det	0.16	0.15	0.00	0.02	0.03	0.00
Kril to Det	0.02	0.01	0.00	0.24	0.39	0.00
Pen to Det	0.00	0.00	0.00	0.00	0.00	0.00
Fish to Det	na	na	na	na	na	na
Exp Phl	0.82	0.67	0.02	9.21	6.22	**0.10**
Exp PhS’	4.20	1.17	**0.12**	18.90	11.69	0.20
Exp Salp	0.01	0.01	0.00	0.00	0.00	0.00
Exp Krill	0.55	0.38	0.02	0.09	0.04	0.00
Exp Pen	0.00	0.00	0.00	0.00	0.00	0.00
Exp Fish	na	na	na	na	na	na
Exp Det	2.61	0.25	**0.08**	2.44	2.43	0.03
Exp DOC	3.24	0.17	**0.09**	8.97	2.38	**0.10**

(To be continued)

(Continued)

South Region	**Negative Chlorophyll anomalies**			**Positive Chlorophyll anomalies**		
Compartment	**Throughput**		**Norm GPP**	**Throughput**		**Norm GPP**
PPlarge	13.07		0.41	69.16		0.60
PPsmall	18.63		0.59	45.68		0.40
Mic	8.63		0.27	22.07		0.19
Kri	6.00		0.19	30.23		0.26
Fish	0.16		0.00	0.15		0.00
Pen	0.08		0.00	0.08		0.00
Det	4.20		0.13	10.97		0.10
DOC	7.19		0.23	25.07		0.22
Bac	4.21		0.13	13.97		0.12
Sal	0.02		0.00	0.47		0.00
Exp	13.60		0.43	38.13		0.33
Flow	**Avg flow**	**SD Flow**	**Norm GPP**	**Avg flow**	**SD flow**	**Norm GPP**
PhyL to mic	0.71	0.38	0.02	3.31	4.11	0.03
PhyS to mic	6.30	3.65	**0.20**	14.89	20.44	**0.13**
Det to Mic	1.18	0.15	0.04	3.18	1.84	0.03
Bac to Mic	0.44	0.52	0.01	0.68	0.77	0.01
DOC to Bac	4.21	0.80	**0.13**	13.97	14.25	**0.12**
PhyL to Lkri	2.54	1.60	**0.08**	19.42	26.89	**0.17**
Mic to kri	2.80	1.13	**0.09**	6.92	8.32	**0.06**
Det to Kri	0.66	0.47	0.02	3.89	3.87	0.03
PhyS to sal	0.01	0.02	0.00	0.33	0.46	0.00
Mic to sal	0.01	0.01	0.00	0.12	0.12	0.00
Det to Sal	0.00	0.00	0.00	0.01	0.01	0.00
Bac to Sal	0.00	0.00	0.00	0.01	0.01	0.00
Kri to Pen	0.04	0.00	0.00	0.04	0.00	0.00
Fish to pen	0.04	0.00	0.00	0.04	0.00	0.00
Kri to fish	0.16	0.01	0.00	0.15	0.01	0.00
Resp phL	3.39	1.63	**0.11**	17.50	22.65	**0.15**
Resp phS	4.96	1.71	**0.16**	12.40	12.68	**0.11**
Resp bac	2.00	0.80	**0.06**	11.76	14.25	**0.10**
Resp mic	3.09	1.19	**0.10**	8.12	9.50	**0.07**
Resp sal	0.01	0.01	0.00	0.22	0.28	0.00
Resp kri	4.52	2.05	**0.14**	26.60	28.05	**0.23**
Resp pen	0.06	0.00	0.00	0.06	0.00	0.00

(To be continued)

(Continued)

Resp Fish	0.06	0.00	0.00	0.06	0.00	0.00
PhL to DOC	2.34	1.02	**0.07**	10.97	13.32	**0.10**
PhS to DOC	2.01	1.61	**0.06**	7.12	6.75	**0.06**
Bac to DOC	0.57	0.26	0.02	0.42	0.44	0.00
Mic to DOC	0.99	0.35	0.03	2.49	2.82	0.02
Sal to DOC	0.00	0.00	0.00	0.07	0.10	0.00
Kri to DOC	0.72	0.18	0.02	3.32	3.38	0.03
Pen to DOC	0.01	0.00	0.00	0.01	0.00	0.00
Fish to DOC	0.02	0.00	0.00	0.02	0.00	0.00
Det to DOC	0.52	0.03	0.02	0.64	0.17	0.01
PhL to Det	0.49	0.26	0.02	1.59	0.25	0.01
PhS to Det	0.49	0.24	0.02	3.57	4.25	0.03
Bac to Det	1.20	0.68	0.04	1.09	1.20	0.01
Mic to Det	1.75	0.50	**0.06**	4.42	4.86	0.04
Salp to Det	0.01	0.01	0.00	0.17	0.22	0.00
Kril to Det	0.21	0.40	0.01	0.08	0.11	0.00
Pen to Det	0.01	0.00	0.00	0.01	0.00	0.00
Fish to Det	0.03	0.01	0.00	0.03	0.00	0.00
Exp Phl	3.59	1.52	**0.11**	16.38	5.24	**0.14**
Exp PhS’	4.86	0.40	**0.15**	7.36	8.74	**0.06**
Exp Salp	0.00	0.00	0.00	0.01	0.01	0.00
Exp Krill	0.35	0.20	0.01	0.03	0.02	0.00
Exp Pen	0.00	0.00	0.00	0.00	0.00	0.00
Exp Fish	0.00	0.00	0.00	0.00	0.00	0.00
Exp Det	1.82	1.19	**0.06**	3.24	4.36	0.03
Exp DOC	2.98	0.74	**0.09**	11.10	11.51	**0.10**